Supplementary Material A: RTK-GNSS measurement quality

Table S1: Coordinate quality (CQ) and occupation details of the RTK-GNSS measurements used for comparison to UAV LiDAR data.

Field site	GNSS Point Type	Occupation Time	Coordinate Quality Type	Mean (m)	Standard Deviation (m)
Garscube	Ground Control Targets	30 s	Horizontal (2D) CQ	0.005	0.001
			Vertical (1D) CQ	0.008	0.002
	Football Pitch markings	5 s	Horizontal (2D) CQ	0.008	0.002
			Vertical (1D) CQ	0.012	0.003
Feshie	Ground Control Targets	1 min	Horizontal (2D) CQ	0.004	0.001
			Vertical (1D) CQ	0.006	0.002
	Road Orthometric Height	5 s	Horizontal (2D) CQ	0.009	0.005
			Vertical (1D) CQ	0.014	0.007
	River Gravel Orthometric Height	5 s	Horizontal (2D) CQ	0.006	0.002
			Vertical (1D) CQ	0.011	0.002
	TLS Targets	Minimum 5 mins	Horizontal (2D) CQ	0.0002	0.0001
			Vertical (1D) CQ	0.0006	0.0004
	Vegetation Orthometric Height	1s	Horizontal (2D) CQ	0.007	0.012
			Vertical (1D) CQ	0.004	0.008

Supplementary Material B: Distribution of M3C2 differences (individual sub-areas)

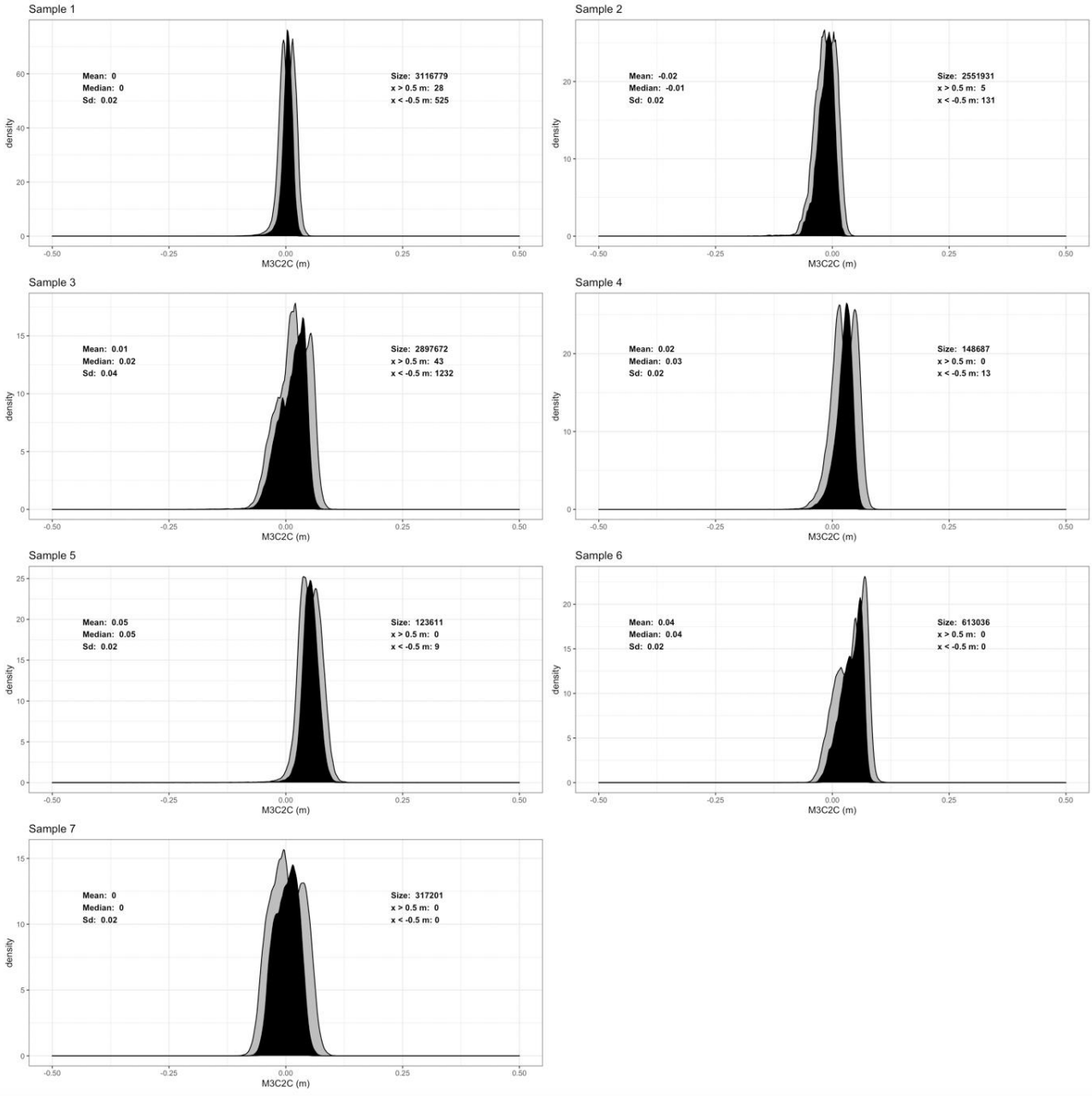

Figure S1: The distribution of the sampled M3C2 differences (Samples 1-7) between the UAV-LiDAR and the TLS point clouds (River Feshie, black). The grey histograms demonstrate the maximum and the minimum expected distributions (M3C2-uncertainty and M3C2+uncertainty for left and right respectively).

Supplementary Material C: Distribution fitting for the combined M3C2 sample (River Feshie).

Figure S2 shows the Cullen and Frey diagram for the identification of candidate distributions for the combined M3C2 sample. The bootstrapped samples fall in the "symmetric" region, and we test the normal and the Cauchy distributions, as the histogram indicates a mean and a median approximating 0. The normal distribution outperforms the Cauchy at the tails of the distributions (Q–Q plot, Figure S3). However, the Cauchy distribution outperforms the normal in terms of central tendency (P–P plot, Figure S3). The histogram and CDF diagrams lead to the same conclusions. The confirmation for the selection of the distribution comes from the goodness of fit criteria (Table S2) where the selected distribution (Cauchy) marginally outperforms the normal for both the Akaike's and the Bayesian calculation.

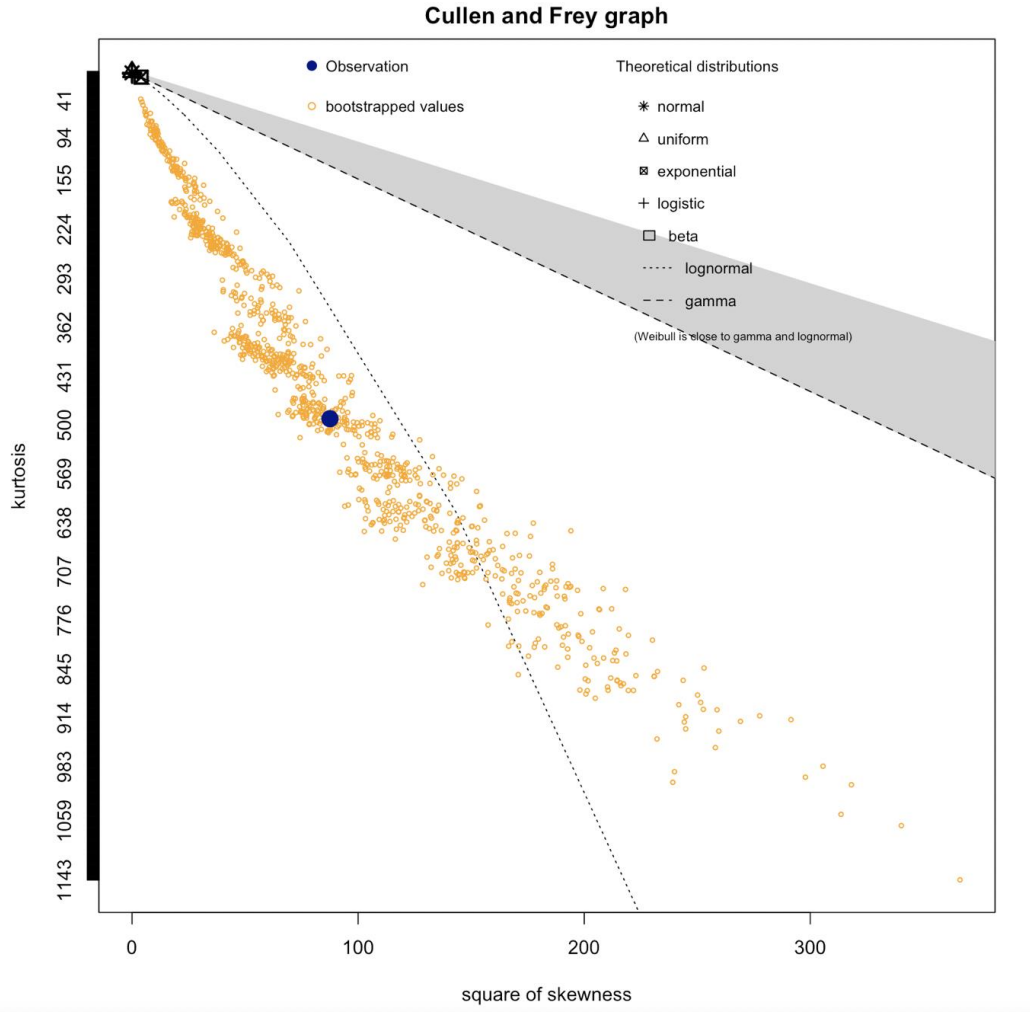

Figure S2: Cullen and Frey diagnostics for the combined M3C2 sample. The area variation of bootstrapped values (yellow) indicates that the best candidate distributions less likely to be non-symmetric. This is supported graphically by the form of the histogram (Figure S3).

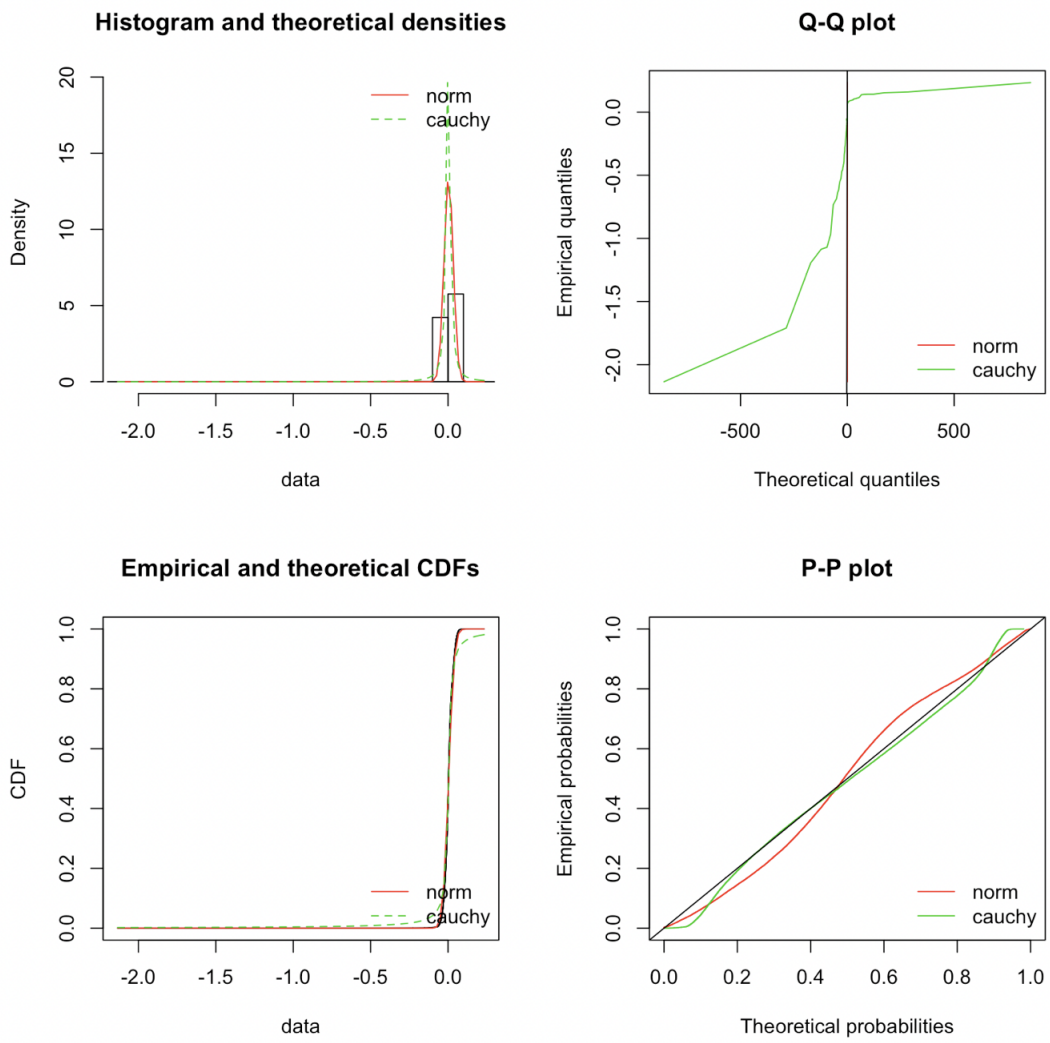

Figure S3: Fitting plots for the examined normal and Cauchy distributions.

Table S2: Goodness of fit statistics for the tested normal and Cauchy distributions. The Cauchy distribution outperforms the normal (marginally) as both the Akaike's and the Bayesian criteria are smaller.

Goodness-of-fit statistics		
	Normal	**Cauchy**
Kolmogorov-Smirnov statistic	0.06752856	0.06044401
Cramer-von Mises statistic	186.06562228	60.54967189
Anderson-Darling statistic	Inf	851.88017587
Goodness-of-fit criteria		
	Normal	**Cauchy**
Akaike's Information Criterion	-420356.9	-425859.6
Bayesian Information Criterion	-420337.8	-425840.6

Figure S4 demonstrates the stability of the selected distribution for M3C2 combined sample. For the Cauchy distribution 1000 bootstrapped parameters were cross compared, revealing a variation of approximately 0.003 for the location parameter and 0.013 for the scale parameter. This range is also confirmed in Table S3, where 97.5% of the bootstrapped parameters fall within those ranges. The differences are marginal, indicating good stability of the selected distribution for the scaling of the data.

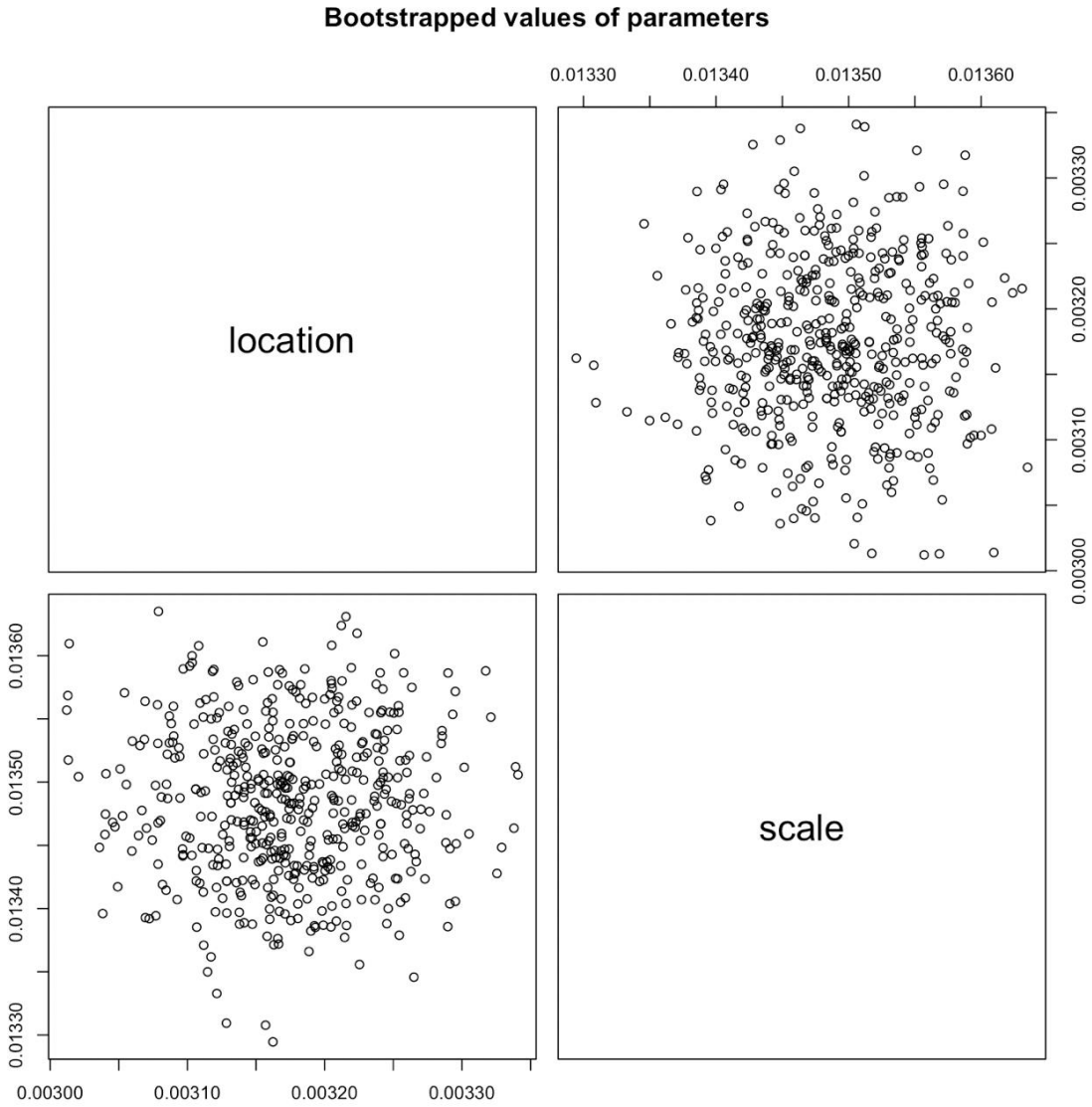

Figure S4: Bootstrap parameters for selected distributions.

Table S3: Statistics of the bootstrapped distribution parameters (Cauchy).

	Median	**2.5%**	**97.5%**
Location	0.003171376	0.003050031	0.00329234
Scale	0.013484919	0.013376707	0.01359002